Translational Oncology 14 (2021) 100895

Contents lists available at ScienceDirect

Translational Oncology

journal homepage: www.elsevier.com/locate/tranon

Original research

Proteomic analysis reveals distinctive protein expression patterns of thrombus in clear cell renal cell carcinoma

Juntuo Zhou [a,b,1], Yimeng Song [a,1], Tianying Xing [a,c], Liyuan Ge [a], Lulin Ma [a], Min Lu [d,*], Lijun Zhong [e,**]

[a] Department of Urology, Peking University Third Hospital, Beijing 100191, China
[b] Beijing Advanced Innovation Center for Big Data-Based Precision Medicine, Beihang University, Beijing 100083, China
[c] Xuanwu Hospital, Capital Medical University, Beijing 100053, China
[d] Department of Pathology, Peking University Third Hospital, School of Basic Medical, Science Peking University Health Science Center, Beijing 100191, China
[e] Medical and Health Analytical Center, Peking University Health Science Center, Beijing 100191, China

ARTICLE INFO

Article history:
Received 26 July 2020
Received in revised form 15 September 2020
Accepted 15 September 2020

Keywords:
ccRCC
tumor thrombus
proteomics
bioinformatics
survival analysis

ABSTRACT

Clear cell renal cell carcinoma (ccRCC) is a type of malignant tumor of the urinary system. The renal vein or vena cava thrombus can be found in a subset of ccRCC patients in whom it leads to worse prognosis. However, the protein expression profile and molecular features of ccRCC thrombus remain largely unclear. Here, a comparative proteomic analysis was performed using the 2D-LC-MS strategy for the thrombus-tumor-normal tissue triples of 15 ccRCC patients. Statistical analysis, GO enrichment analysis, protein-protein interaction network construction, and mRNA-based survival analysis were used to interpret the proteomic data. Three dysregulated proteins, GGT5 (gamma-glutamyl transferase 5), KRT7 (keratin 7) and CFHR1 (complement factor H related 1), were analyzed using western blot (WB) and immunohistochemistry (IHC) to validate the reliability of the proteomic analysis. The result of this analysis revealed 251 dysregulated proteins, which could be divided into 11 clusters depending on the changing trends, among the thrombus, tumor, and normal tissues. Several pathways and regulation networks were found to be associated with the thrombus, and some dysregulated proteins showed potential values for prognosis prediction. WB and IHC results were in accordance with the proteomic results, further validating the reliability of this study. In conclusion, our findings provide an overview of the thrombus at the molecular level as well as valuable information for further pathological studies or research on biomarkers and therapeutic targets.

Introduction

Clear cell renal cell carcinoma (ccRCC), originating from the epithelial system of the uriniferous tubule in the renal parenchyma, is a malignant tumor of the urinary system [1,2]. Approximately 2%–3% of adult malignant tumors are RCCs, of which 4%–10% invade the venous system, forming a renal vein or inferior vena cava thrombus [3,4]. Patients with ccRCC who also have a vena cava thrombus, exhibit poor prognosis, and there is no clear pathogenesis for its development at present [5,6]. Thus, there is an urgent need to investigate the protein expression profiles in thrombus and to compare it with the protein expression profiles in the tumor and normal tissues, to understand the special biological features of the thrombus.

Some previous studies have been performed to explore the features of the tumor thrombus. Paranita and colleagues profiled the genomes and transcriptomes of the primary ccRCC tumor, thrombus, and lung metastases, finding several perturbed genes mainly located in the extracellular matrix between primary tumors and thrombus [7]. Moreover, Xiangming and colleagues applied whole-exome sequencing and transcriptome sequencing of ccRCC tumor and thrombus tissue samples, and found distinct molecular characteristics in patients with or without thrombus [8]. In a study by Michael and colleagues, immune-cell enumeration and programmed death-ligand 1 (PD-L1) expression analysis in ccRCC patients with tumor thrombus, thrombus had higher levels of M1 macrophages, but the PD-L1 expression analysis on ccRCC biopsy did not represent its corresponding thrombus [9]. Moreover, Michael and colleagues performed a microbiome evaluation and PD-L1 expression profiling in ccRCC patients with associated tumor thrombus, and found that the tumor thrombus was mostly devoid of diverse microbiota [10]. These studies showed the genomic and immunogenic heterogeneity of the thrombi compared to that of primary tumors. However, the protein expression profile of the thrombus, which would provide valuable information for its molecular features, has not been reported.

* Corresponding author.
** Correspondence to: L. Zhong, Center of Medical and Health Analysis, Peking University Health Science Center, Beijing, China; Peking University Health Science Center, Beijing 100191, China.
E-mail addresses: lumin@bjmu.edu.cn, (M. Lu), zhonglijun@bjmu.edu.cn. (L. Zhong).
[1] Juntuo Zhou and Yimeng Song contribute equally to this work.

http://dx.doi.org/10.1016/j.tranon.2020.100895

Proteomics, as a rapidly developing protein profiling strategy, and it has been widely applied in biological mechanism- and clinical application-related studies. Furthermore, it has shown great advantages, including wide proteome coverage and ideal analytical robustness [11,12]. In this study, we performed label-free proteomic analysis of the thrombus, tumor, and normal tissues of ccRCC patients to provide a comprehensive view of the protein expression profiles. Further statistical, bioinformatics, and mRNA-based survival analyses revealed distinctive molecular features of the thrombus, providing novel targets for pathological research or drug development.

Materials and methods

Materials

Tris-(2-carboxyethyl) phosphine (TCEP) was acquired from Thermo Scientific (Rockford, Il, USA). Ammonium bicarbonate (NH_4HCO_3) and iodoacetamide (IAA) were purchased from Sigma (St. Louis, MO, USA). Sequencing-grade trypsin was purchased from Promega (Madison, WI, USA). All mobile phases were prepared with HPLC grade solvents (i.e. formic acid, water, and acetonitrile) from Sigma Aldrich. All other reagents were of standard biochemical quality.

Patients and specimens

Patients were included who had histologically confirmed ccRCC and received no treatments before surgery. Primary ccRCC tissues, matched thrombus tissues and adjacent morphologically normal kidney tissues or adjacent normal tissues from the same patient were collected from 15 patients with ccRCC and nephrectomy at Peking University Third Hospital. This study was approved by local ethics committees (Peking University Third Hospital) with the ethical approval code of M2017147, and written informed consent was obtained from all patients.

Sample preparation

Total protein of ccRCC tissues, thrombus tissues and normal kidney tissues was extracted and processed as previously described [13]. In brief, tissue samples were homogenized in RIPA lysis buffer (Millipore, Billerica, MA, USA) containing the protease inhibitor cocktail (Roche, Basel, Switzerland). Protein was collected through centrifugation at 12,000 $\times g$ for 10 min at 4 ˚C and protein concentration was determined with a BCA protein assay (Thermo, IL, USA). Sample pooling procedure was done by combining 5 samples into 1 pooled sample and lead to three biological replicates in each group (Tumor, thrombus and normal tissue). Protein digestion was conducted by FASP [14] using Amicon Ultra-4 10k centrifugal filters (Merck Millipore, Ireland). 200 μg total protein of each replicate was denatured with 8 M urea in 0.1 M Tris/HCl (pH 8.5) and then processed with 0.05 M TCEP and 0.1 M iodoacetamide (IAA) in sequence. Finally, trypsin was added at an enzyme to protein ratio of 1:50 in 50 mM NH_4HCO_3 solution at 37 ˚C overnight. The released peptides were collected through centrifugation and dried by vacuum.

2D-LC based proteomic analysis

2D-LC-MS based proteomic analysis was performed as previously described [13]. Firstly, high pH reverse phase chromatography was performed using the Dionex Ultimate 3000 Micro Binary HPLC Pump system. The digested peptide mixture was reconstituted with mobile phase A (20 mM ammonium formate in water, pH 10) and then separated using a 2.1 mm × 150 mm Waters BEH130 C-18 column at a flow rate of 230 μL/min. The gradient was 5% mobile phase B (20 mM ammonium formate in 80% acetonitrile, pH 10) for 5 min, 5% to 15% B for 15 min, 15% to 25% B for 10 min, 25% to 55% B for 10 min, and 55% to 95% B for 5 min. Elution was monitored by measuring the absorbance at 214 nm, and 15 fractions were collected based on peptide density and vacuum-dried.

LC-MS analysis was performed on a nano-flow HPLC system (Easy-nLC II, Thermo Fisher Scientific, Waltham, MA, USA) connected to an LTQ-Orbitrap Velos Pro mass spectrometer (Thermo Fisher Scientific). Chromatographic separation was performed on a reversed phase C18 column (Easy-column C18-A2, 75 μm I.D. × 100 mm, 3 μm, Thermo Fisher Scientific) at a flow rate of 300 nL/min with a 60 min gradient of 2% to 40% acetonitrile in 0.1% formic acid. The LTQ-Orbitrap was operated in data-dependent mode to measure full scan MS1 spectra (m/z 300–1800) in the Orbitrap with a mass resolution of 60,000 at m/z 400. After MS1 survey, the 15 most abundant ions detected in the MS1 scan were measured in MS2 scans using collision-induced dissociation (CID).

Protein identification and quantification

Protein identification and label-free quantitation were performed with MaxQuant version 1.5.1.6 using default setting if not stated otherwise. False-discovery rate (FDR) at the peptide and protein level was set to 0.01. Oxidized methionine (M) and acetylation (protein N-term) were selected as variable modifications, and carbamidomethyl (C) as fixed modification. Maximum of two missed cleavages was allowed. Min count ratio for LFQ was set to 2. Match between runs function was enabled and set to 2 min. Database searching was performed against the UniProt FASTA database (Human proteome, downloaded in 2018, 20,399 entries). After protein identification and quantitation, data filtering and processing were performed using Perseus software. The identified proteins were filtered for at least 100% valid values (3 biological replications) in at least one group (tumor, thrombus or normal tissue).

Bioinformatic analysis

Principal component analysis score plot and hierarchical clustering-based heat map were drawn using MetaboAnalyst web service (https://www.metaboanalyst.ca/). Gene Ontology (GO) and KEGG pathway enrichment analysis, and protein to protein interaction network construction were performed using the Metascape web service (https://metascape.org/gp/index.html) with the dysregulated proteins used as input. For GO and KEGG enrichment result presenting, a subset of enriched terms was selected and rendered as a network plot, where terms with a similarity > 0.3 were connected by edges. Enriched terms were grouped to clusters by similarity, and the terms with the best p-values from each clusters was shown by name. For protein to protein interaction network construction, analysis was carried out with the following databases: BioGrid, InWeb_IM, and OmniPath. The resultant network contained the subset of proteins that form physical interactions with at least one other member in the list. The Molecular Complex Detection (MCODE) algorithm was applied to identify densely connected network components. Pathway and process enrichment analysis was applied to each MCODE component independently, and the best-scoring term by p-value was retained as the functional description of the corresponding components. TCGA database based survival analysis was performed using the GEPIA2 web service (http://gepia2.cancer-pku.cn/#index), the method was set to Disease Free Survival (RFS) analysis, and other parameters were set as default.

Western blot analysis

Western blot (WB) analysis was performed according to standard protocols. In brief, 40 μg of the total protein was electrophoretically separated on a 10% SDS-PAGE gel. The proteins were then transferred to a PVDF membrane and probed with primary antibodies: anti-CFHR1 (1,1000; Abcam, Cambridge, MA), anti-KRT7 (1,1000; Bioworld Technology, Minneapolis, MN), anti-GGT5 (1,1000; Bioworld Technology, Minneapolis, MN, USA), and anti-β-actin (1,1000; Santa Cruz Biotechnology, Santa Cruz, CA). Protein expression was visualized after the membrane was incubated with secondary antibodies conjugated with horseradish peroxidase and enhanced chemoluminescence reagent (Santa Cruz Biotechnology, Santa Cruz, CA). The intensity of protein staining was determined using NIH Image J

software after gray scanning. Average protein expression was calculated using the WB results of 15 patients in the validation cohort.

Immunohistochemical staining

Samples were processed for hematoxylin-eosin staining (H&E staining) and IHC by routine techniques. Briefly, deparaffinized tissue sections were incubated with 3% hydrogen peroxide for 10 min at 37 ˚C. Tissue sections were then placed in 0.01 M citrate antigen retrieval solution (pH 6.0), heated at 95 ˚C in a microwave oven for 10 min and cooled to room temperature. Slides were reacted for 2 h at room temperature with primary rabbit polyclonal antibody to CFHR1 (Abcam; Rabbit; 1:500 dilution), KRT7 (Bioworld; Rabbit; 1:500 dilution), GGT5 (Bioworld; Rabbit; 1:500 dilution). Secondary antibodies conjugated with horse-radish peroxidase (rabbit; DAKO, Denmark) were incubated for 40 min at RT, followed by incubation with the substrate 3, 3′ diaminobenzidine (DAKO, Denmark) before counterstaining with Mayer hematoxylin. For negative controls, primary antibodies were omitted from the dilution buffer. Granular cytoplasmic staining of CFHR1, GGTS and KRT7 were considered to be positive.

Statistical analysis

For dysregulated proteins screening form proteomic data, the significance was determined by ANOVA with Fisher's LSD post-hoc comparison, and a protein with an FDR adjusted p value < 0.05 and a fold change > 2 was considered dysregulated between groups. For statistical analysis of WB results, the significance of variability was determined by ANOVA with post-hoc comparison, with Student's *t*-test for continuous variables and by chi-square or Fisher's exact test for nominal variables, as appropriate. All data are presented as mean ± SD from at least three independent experiments. $p < 0.05$ was considered statistically significant.

Data availability

The raw MS data and MaxQuant processed result were deposited in MassIVE database with ID: MSV000085727.

Results

Overview of the proteomic workflow

This study aimed to explore the protein expression profiles of ccRCC tumor and thrombus compared to normal kidney tissue. The schematic flowchart of the proteomic workflow and the results are shown in Fig. 1A. Three sample groups (tumor, thrombus, and normal) derived from 15 ccRCC patients (Table 1) were collected and analyzed by label-free proteomics. A total of 5416 proteins were identified with confidence and 3631 proteins were detected in all three biological replicates in at least one group. ANOVA p value and fold-change-based screening revealed 251 dysregulated proteins among groups. Next, PPI network construction, GO enrichment analysis, and survival analysis further revealed the relevant perturbed pathways in the thrombus or tumors. Finally, three dysregulated proteins were analyzed via WB and IHC to validate the reliability of the proteomic results. This result provided dysregulated proteins and perturbed pathways in the ccRCC thrombus and tumor, which helped to gain an overview of the distinct characteristics of these two subtypes at the molecular mechanism level.

Proteins dysregulated between tumor, thrombus, and normal tissues

The protein expression profiles were first overviewed by the PCA score plot (Fig. 1B), in which the normal group presented a clear distinction from tumor and thrombus, and differences were also observed between the thrombus and tumor groups. Further ANOVA and fold change-based screening revealed a total of 251 dysregulated proteins among the three sample groups (Table S1), and 13 of them were found to be dysregulated between each group (thrombus vs. tumor, thrombus vs. normal, and tumor vs. normal). The expression levels of the 13 proteins are shown in the heat map in Fig. 2A, and five clusters (cluster 1–5) could be found according to the change trends (Fig. 2A and B). The GO terms of these 13 proteins are shown in Table 2.

Proteins solely dysregulated in thrombus or tumor tissue

Among the dysregulated proteins, 4 proteins (MMP7, PLXNB1, ERLIN1, and YARS2) were found to be downregulated (cluster 6) or upregulated (cluster 7) in the thrombus, with no difference between tumor and normal tissue (Fig. 3A). Twenty-nine proteins were found only upregulated (cluster 8) or downregulated (cluster 9) in the tumors, with no difference between the thrombus and normal tissue (Fig. 3B). The change trends of the clusters (clusters 6–9) are shown in Fig. 3C. The results of GO and pathway enrichment analysis using proteins in clusters 8 and 9 are shown in Fig. 3D. Several GO terms were significantly enriched, such as aspartate family amino acid metabolic process, leukocyte degranulation, and cell adhesion molecule binding.

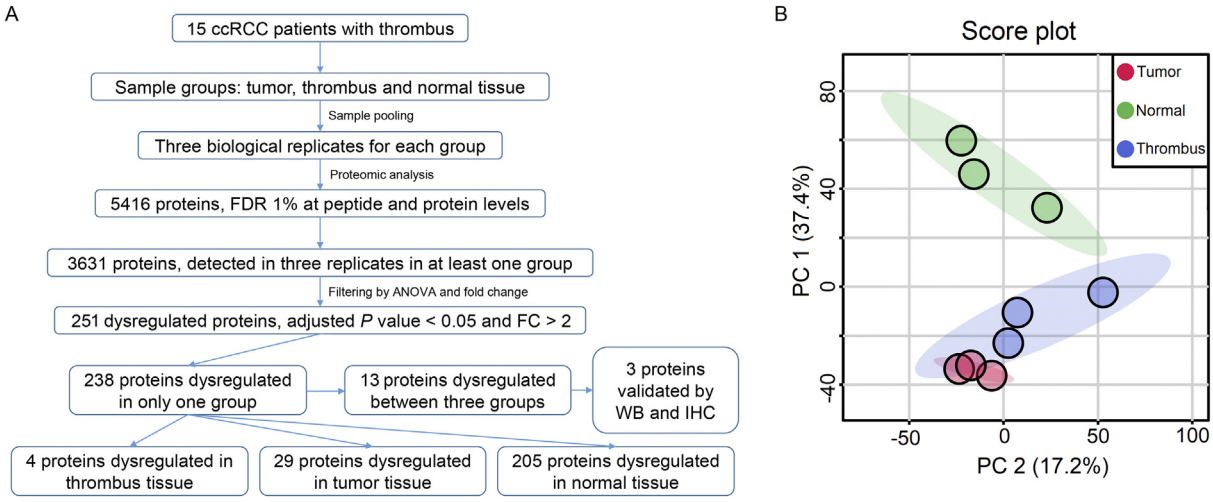

Fig. 1. Overview of the proteomic workflow and result. (A) Schematic flowchart of the proteomic study and result. (B) Score plot of the PCA representing the distribution of samples in term of protein expression profiles. Sample groups were marked by colors.

Table 1
Clinicopathologic characteristics of the ccRCC patients with thrombus.

Cohort	Case no.	Sex	Age	WHO/ISUP grading system	TNM
Discovery	1	F	54	4	pT3bN1M1
Discovery	2	M	59	2	pT3bN0M1
Discovery	3	F	61	3	pT3bN0M0
Discovery	4	M	70	3	pT3cN0M0
Discovery	5	M	61	2	pT3cN0M0
Discovery	6	F	55	4	pT3bN1M0
Discovery	7	M	76	4	pT3bN1M1
Discovery	8	M	82	2	pT3aN0M0
Discovery	9	F	69	3	pT3cN1M1
Discovery	10	M	76	3	pT3bN0M0
Discovery	11	M	56	2	pT3bN0M0
Discovery	12	F	64	2	pT3bN0M0
Discovery	13	M	62	3	pT3aN0M0
Discovery	14	M	76	2	pT3bN1M0
Discovery	15	F	62	1	pT3bN1M1
Validation	1	M	58	3	pT3cN0M1
Validation	2	F	29	4	pT3bN1M0
Validation	3	M	78	3	pT3bN0M1
Validation	4	F	47	2	pT3aN0M0
Validation	5	M	68	4	pT3bN0M0
Validation	6	M	46	3	pT3aN0M0
Validation	7	M	78	3	pT3aN0M0
Validation	8	M	64	2	pT3aN1M0
Validation	9	F	67	1	pT3aN0M0
Validation	10	M	59	2	pT3aN0M0
Validation	11	M	65	2	pT3aN0M0
Validation	12	F	67	2	pT3aN0M0
Validation	13	F	48	2	pT3aN0M0
Validation	14	M	57	4	pT3aN1M0
Validation	15	F	53	1	pT3aN0M0

Proteins solely dysregulated in normal tissue

Among the total dysregulated proteins, 205 proteins were found to be upregulated (cluster 10) or downregulated (cluster 11) in normal tissue, with no difference found between the thrombus and tumor tissues (Fig. 4A). The change trends of the clusters (clusters 10 and 11) are shown in Fig. 4B. The results of GO and pathway enrichment analysis using proteins in clusters 10 and 11 are shown in Fig. 4C. Several GO terms were significantly enriched, such as small molecule catabolic process, organic cyclic compound catabolic process, and monocarboxylic acid metabolic process.

PPI networks of the dysregulated proteins

To further reveal the regulative patterns in ccRCC disease progression, PPI network construction and MCODE-based sub-clustering were performed (Fig. 5A). A total of 6 MCODE sub-networks were found, and their change trends were marked (Fig. 5B). Most of the proteins in MCODE sub-networks, except DCN, belonged to dysregulated protein clusters 10 and 11, which means that these proteins were only dysregulated in the normal tissue, without differences between the thrombus and tumor tissues. Five GO terms, such as protein targeting to ER, response to endoplasmic reticulum stress, and small molecule catabolic process, were enriched for the MCODE sub-networks, as presented in Fig. 5B.

Survival analysis

To explore the potential relationship between dysregulated proteins and prognosis of ccRCC patients, survival analysis was performed using transcriptome data and clinical follow-up information from the TCGA database. In addition to ccRCC, we included some other types of urinary tumors and common types of tumors in the survival analysis, such as kidney renal papillary cell carcinoma, bladder urothelial carcinoma, liver hepatocellular carcinoma, and lung adenocarcinoma, to gain an overview of the specificity of these dysregulated proteins in the ccRCC. The results are presented as heat maps for dysregulated protein cluster 10 (Fig. 6A), cluster 11 (Fig. 6B), clusters 6–7 (Fig. 6C), clusters 1–5 (Fig. 6D), and clusters 8–9 (Fig. 6E). The K-M survival curves of two representative proteins (PHYHD1 and CHDH) are shown in Fig. 6F–G.

Validation of dysregulated proteins, KRT7, GGT5, and CFHR1

To validate the reliability of the proteomic results, we chose three dysregulated proteins (KRT7, GGT5, and CFHR1) from the dysregulated

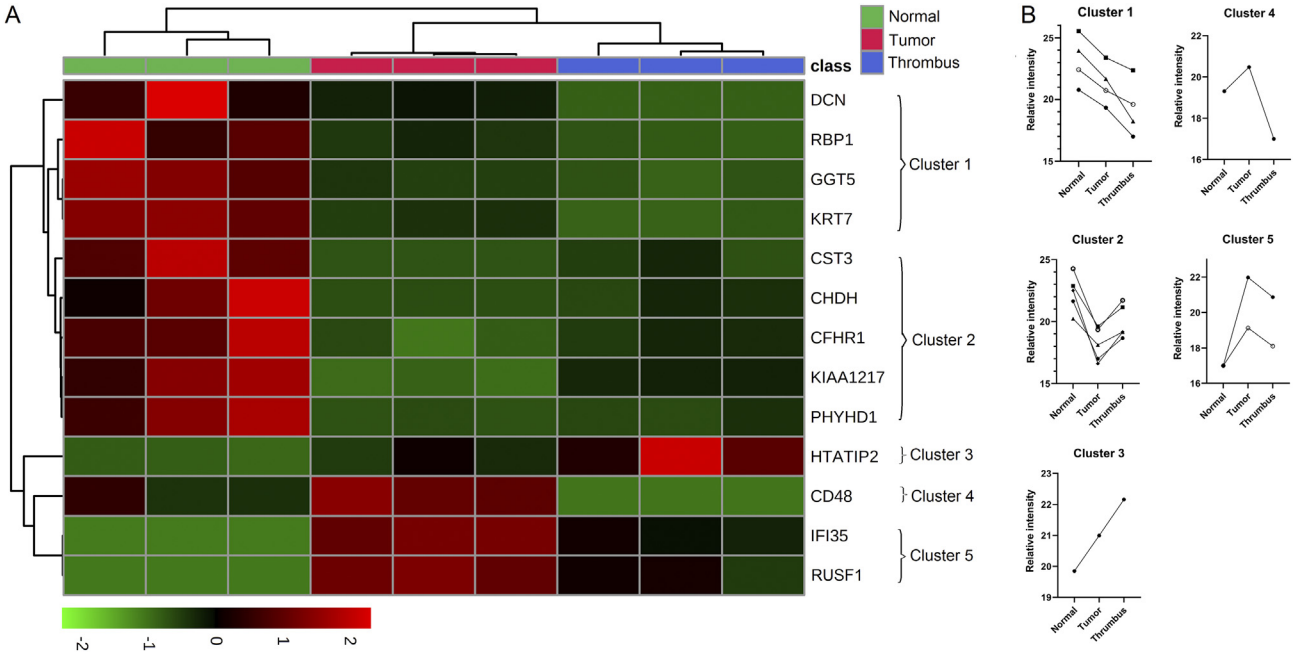

Fig. 2. Proteins dysregulated among thrombus, tumor and normal tissue. (A) Hierarchical clustering heat map presenting the expression profiles of the proteins dysregulated among thrombus, tumor and normal tissue. 5 clusters could be found according to regulative trends. (B) Line chart presenting the regulative trends of the dysregulated proteins in cluster 1–5. Each line represented a protein and the average intensity of each protein from the three biological replicates was used.

Table 2
The GO enrichment results of the proteins in cluster 1–5.

Gene symbol	Description	Biological process (GO)	Cellular component (GO)	Molecular function (GO)
DCN	Decorin	Dermatan sulfate biosynthetic process; negative regulation of vascular endothelial growth factor signaling pathway; chondroitin sulfate catabolic process	Collagen type VI trimer; collagen beaded filament; lysosomal lumen	Extracellular matrix structural constituent conferring compression resistance; collagen binding; extracellular matrix binding
CD48	CD48 molecule	Regulation of adaptive immune response; leukocyte migration; adaptive immune response	Membrane raft; membrane microdomain; extracellular exosome	Antigen binding; signaling receptor activity; molecular transducer activity
RBP1	Retinol binding protein 1	Retinoic acid biosynthetic process; vitamin A metabolic process; retinoic acid metabolic process	Lipid droplet; nucleoplasm; nuclear lumen	All-trans-retinol binding; retinol binding; retinal binding
IFI35	Interferon induced protein 35	Type I interferon signaling pathway; cellular response to type I interferon; response to type I interferon	Cytosol; nucleus; cytoplasmic part	Protein binding; binding
GGT5	Gamma-glutamyltransferase 5	Leukotriene D4 biosynthetic process; leukotriene D4 metabolic process; leukotriene biosynthetic process	Intrinsic component of plasma membrane; plasma membrane part; plasma membrane	Leukotriene-C(4) hydrolase; hypoglycin A gamma-glutamyl transpeptidase activity; leukotriene C4 gamma-glutamyl transferase activity
RUSF1	RUS family member 1		Integral component of membrane; intrinsic component of membrane; membrane part	Protein binding; binding
KIAA1217	KIAA1217	Embryonic skeletal system development; chordate embryonic development; skeletal system development	Cytoplasm; intracellular part; intracellular	Molecular_function
HTATIP2	HIV-1 Tat interactive protein 2	Regulation of angiogenesis; import into nucleus; angiogenesis	Nuclear envelope; organelle envelope; envelope	Transcription coactivator activity; protein serine/threonine kinase activity; transcription coregulator activity
CHDH	Choline dehydrogenase	Glycine betaine biosynthetic process from choline; choline catabolic process; glycine betaine biosynthetic process	Mitochondrial inner membrane; mitochondrial membrane; organelle inner membrane	Choline dehydrogenase activity; flavin adenine dinucleotide binding; oxidoreductase activity
PHYHD1	Phytanoyl-CoA dioxygenase domain containing 1	Oxidation-reduction process; metabolic process		Dioxygenase activity; oxidoreductase activity; metal ion binding
CST3	Cystatin C	Negative regulation of elastin catabolic process; negative regulation of collagen catabolic process; regulation of elastin catabolic process	Tertiary granule lumen; ficolin-1-rich granule lumen; tertiary granule	Cysteine-type endopeptidase inhibitor activity; amyloid-beta binding; endopeptidase inhibitor activity
CFHR1	Complement factor H related 1	Cytolysis by host of symbiont cells; cytolysis in other organism involved in symbiotic interaction; killing by host of symbiont cells	Blood microparticle; extracellular space; extracellular region part	Identical protein binding; protein binding; binding
KRT7	Keratin 7	Cornification; keratinization; keratinocyte differentiation	Keratin filament; intermediate filament; intermediate filament cytoskeleton	Protein binding; binding; molecular_function

protein clusters 1 and 2, to be analyzed by WB and IHC in an independent patient cohort. Fifteen cases of primary ccRCC with thrombus and their matched adjacent normal kidney tissues were analyzed by WB. As shown by the representative WB results in Fig. 7A, KRT7 and GGT5 were found to be downregulated from normal tissue, tumor tissue to thrombus tissues in a sequence, while CFHR1 was found to be downregulated from normal tissue, thrombus tissue to tumor tissue in a sequence. To generalize the WB results of 15 patients, we calculated the amount of target proteins by gray scanning, and presented the statistical results as a column graph (Fig. 7B). The original images of the WB analysis of all the 15 patients in the validation cohort are presented in the supplementary material (Fig. S1). As shown in the IHC results (Fig. 7C), in normal renal parenchyma, the proximal convoluted tubules and distal tubules were strongly stained with the three antibodies. In detail, KRT7, GGT5, and CFHR1 were expressed in tumor cells less than in the normal parenchyma, or almost negative in the tumor cells. Meanwhile, both KRT7 and GGT5 staining were stronger in the tumor tissues than in thrombus tissues. Unlike KRT7 and GGT5, CFHR1 was more strongly expressed in the thrombus than in the tumors. The change trends of these three proteins in WB and IHC results were in accordance with the proteomic results.

Discussion

For patients with ccRCC, the extent of the tumor thrombus is considered to be associated with the risk of mortality after surgery, and patients whose thrombus extends deep into the vena cava have the worst prognosis [8]. However, the detailed pathological mechanism and molecular features of thrombus are still not fully understood. In this study, we aimed to explore the proteomic profiles of ccRCC tumor and thrombus to provide an overview of the distinctive molecular features of thrombus and tumor. Our findings not only provide valuable clues for pathological research, but also reveal novel targets for diagnostic or therapeutic purposes.

The dysregulated proteins found through proteomic analysis could be divided into 11 clusters, according to their change trends in the thrombus, tumor, and normal tissues. The proteins in clusters 1–5 (Fig. 2) were of great research value because they were dysregulated in all the three groups (thrombus vs. tumor, thrombus vs. normal tissue, and tumor vs. normal tissue), which made them distinctive features for discriminating thrombus, tumor, and normal tissue. Among them, proteins in cluster 1 (DCN, RBP1, GGT5, and KRT7) presented a consecutive downregulation from normal tissue to tumor to thrombus. Decorin (DCN) is a small leucine-rich proteoglycan that stimulates connective tissue collagen synthesis and regulates connective tissue formation in the extracellular region [15,16]. DCN has been reported to suppress growth and tumor angiogenesis by binding EGFR for tumor cell cycle arrest and apoptosis [17]. RBP1 is a retinol-binding protein that also plays a role in the induction of growth, arrest and cellular senescence via mechanisms such as transcriptional repression [18]. Thus, we may infer that the downregulation of DCN and RBP1 plays an important role in tumor and thrombus development. GGT5, a cell surface protein that converts leukotriene C4 (LTC4) to LTD4, is usually expressed in different cell types such as the interstitial cells of the kidney and Kupffer cells in the liver [19], but few studies have focused on the role of GGT5 in tumors. KRT7 (keratin 7), also known as CK7 (cytokeratin 7), is an intermediate filament usually expressed on ductal epithelial cells and bronchial and mesothelial cells but absent in the colon, ectocervix, and liver. Conventionally, KRT7 is usually positive in pRCC (papillary

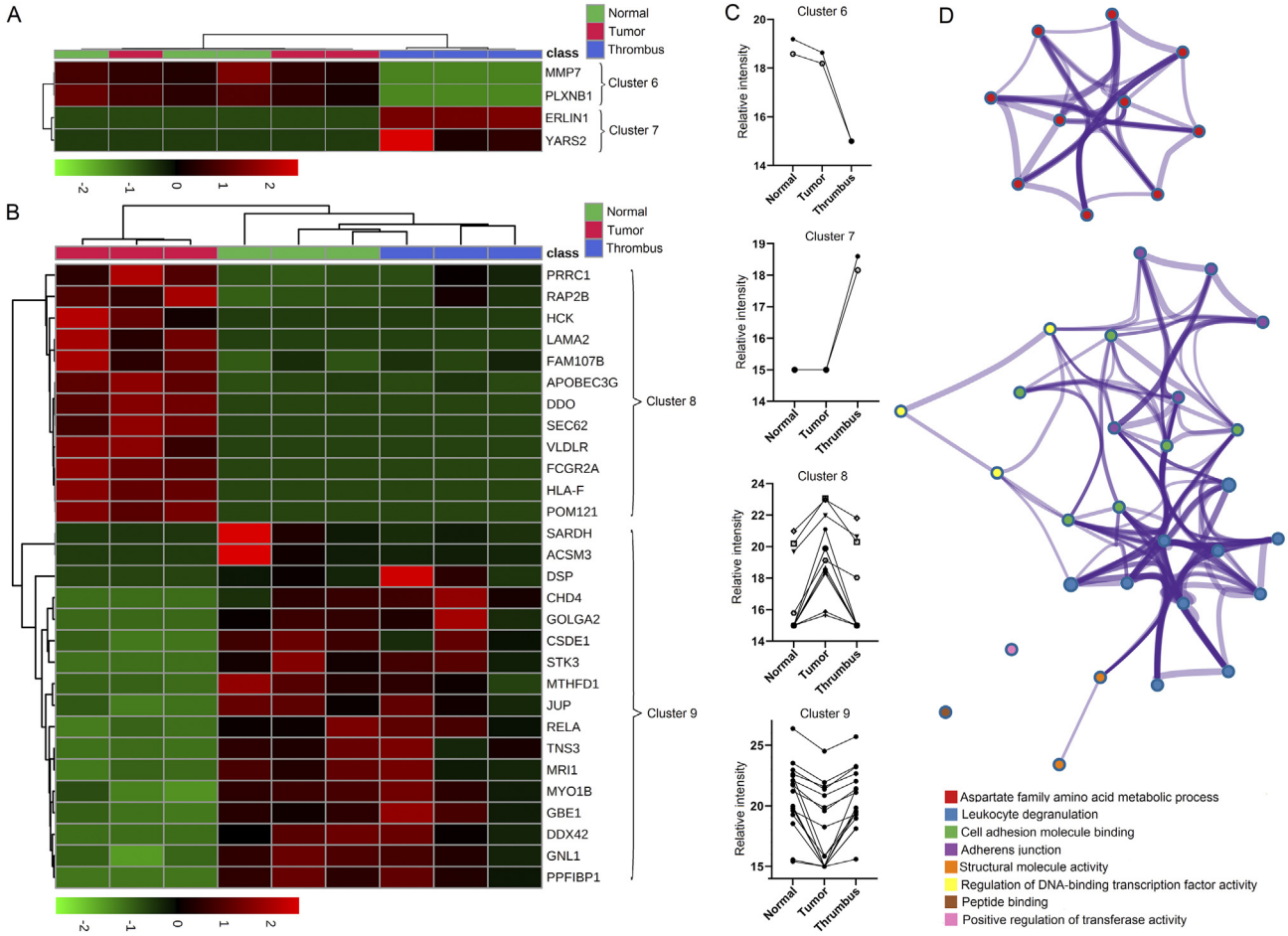

Fig. 3. Proteins dysregulated only in thrombus or tumor. (A) Hierarchical clustering heat map presenting the expression profiles of the proteins dysregulated only in thrombus. 2 clusters could be found according to the regulative trends. (B) Hierarchical clustering heat map presenting the expression profiles of the proteins dysregulated only in tumor. 2 clusters could be found according to the regulative trends. (C) Line chart presenting the regulative trends of the dysregulated proteins in cluster 6–9. Each line represented a protein and the average intensity of each protein from the three biological replicates was used. (D) Network presenting enriched GO terms (nodes). Each node represents an enriched term and is colored first by its cluster ID. For clarity, term labels are only shown for one term per cluster. Terms that share the same cluster ID are typically close to each other.

renal cell carcinoma) and chRCC (chromophobe renal cell carcinoma) but negative in most ccRCC (clear cell renal cell carcinoma) [20]. Our findings reveal a potential relationship between the downregulated GGT5 and KRT7 in ccRCC tumors, especially in the thrombus.

Interestingly, the proteins in clusters 6 and 7 showed distinctive expression patterns compared to normal and tumor tissues (Fig. 3A). MMP7 and PLXNB1 were only weakly expressed in the thrombus, whereas ERLIN1 and YARS2 were only highly expressed in the thrombus. MMP7 and PLXNB1 were located in the extracellular region and regulate invasive growth and cell migration [21,22], which may play an important role in the development of thrombus tissue into veins. These 4 dysregulated proteins may provide clues to the mechanism of the thrombus's distinctive biological behavior and could also be considered as potential markers for thrombus formation. The proteins in clusters 8 and 9 were only up- or downregulated in the tumor tissue, and no difference was observed between the thrombus and normal tissue. This result demonstrates that the thrombus not only exhibits different biological features from general ccRCC tumor, but also may be more likely to act as normal tissues. The GO enrichment results for the proteins in clusters 8 and 9 revealed several relevant terms (Fig. 3D), except that some amino acid-related metabolic processes, several adhesion - and structure-related terms were enriched. These results show the potential mechanism for the distinctive migration or invasion features of thrombus. Proteins in clusters 10 and 11, which were only found to change in normal tissue with no difference found between thrombus and tumor, could be considered as common features shared by tumor and thrombus. Several metabolic and catabolic processes were enriched from these proteins (Fig. 4C), suggesting that these processes were highly relevant to ccRCC derived tumor and thrombus cells.

To better explore the regulatory pathway of the dysregulated proteins, we employed PPI network construction, and employed the MCODE subgrouping algorithm to reveal important regulating protein subgroups that work as a network (Fig. 5). MCODE 1 is mainly composed of ribosomal proteins targeting the endoplasmic reticulum (ER) with functions of translation. These proteins were upregulated in both thrombus and tumor tissue, suggesting the importance of activated translation in the development of both thrombus and tumor. Another valuable sub-network was the DCN-EGFR comprising network (MCODE 2, Fig. 5C). DCN is a proteoglycan that negatively regulates proliferation, migration, and invasiveness of cells [23], while studies have shown that EGFR is usually highly expressed in many solid tumors [24]. Previous studies have also found that DCN could act as a biological ligand for EGFR and modulate cell behavior via EGFR down-regulation [25]. In the present study, DCN was found to be downregulated consecutively from normal tissue to tumor to thrombus, while EGFR was upregulated in thrombus and tumor. This result shows that the DCN-EGFR-related regulatory pathway may play a vital role in thrombus and tumor proliferation or invasion. These sub-networks could help researchers concentrate on the key proteins involved in ccRCC tumor and thrombus tumorigenesis, and could also be considered as candidates for novel marker or drug development.

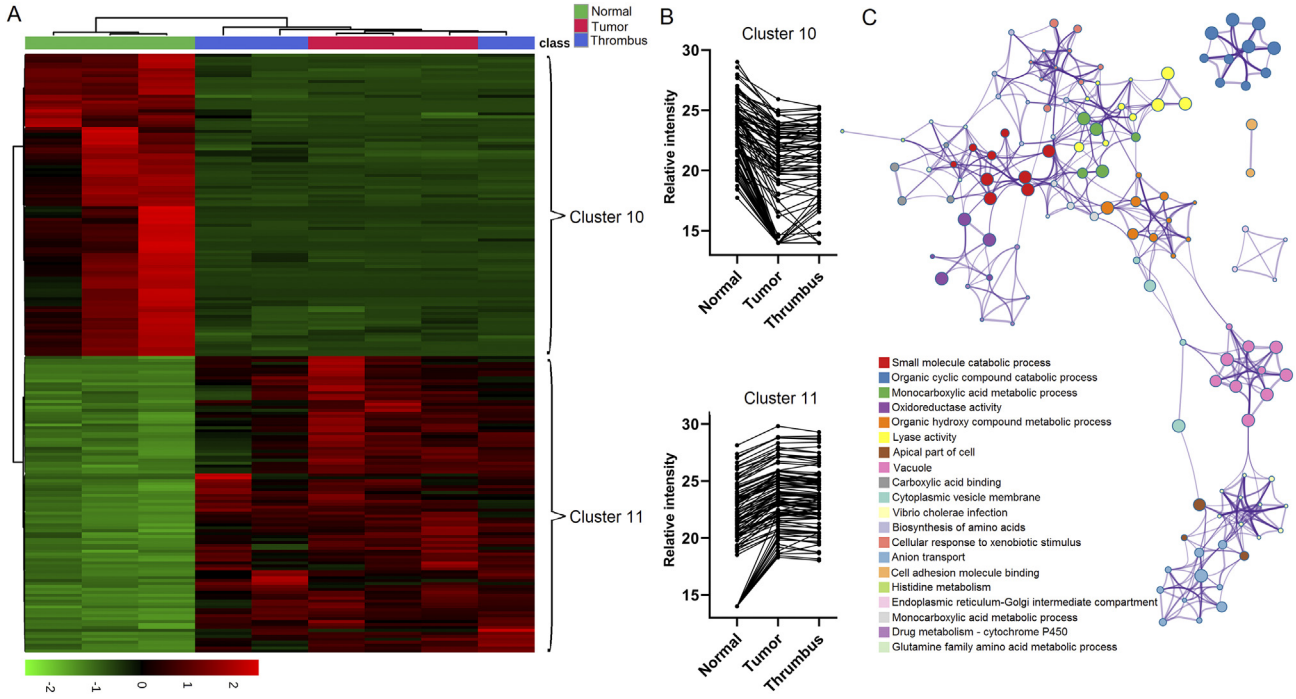

Fig. 4. Proteins dysregulated only in normal tissue. (A) Hierarchical clustering heat map presenting the expression profiles of the proteins dysregulated only in normal tissue. 2 clusters could be found according to the regulative trends. (B) Line chart presenting the regulative trends of the dysregulated proteins in cluster 10–11. Each line represented a protein and the average intensity of each protein from the three biological replicates was used. (C) Network presenting enriched GO terms (nodes). Each node represents an enriched term and is colored first by its cluster ID. For clarity, term labels are only shown for one term per cluster. Terms that share the same cluster ID are typically close to each other.

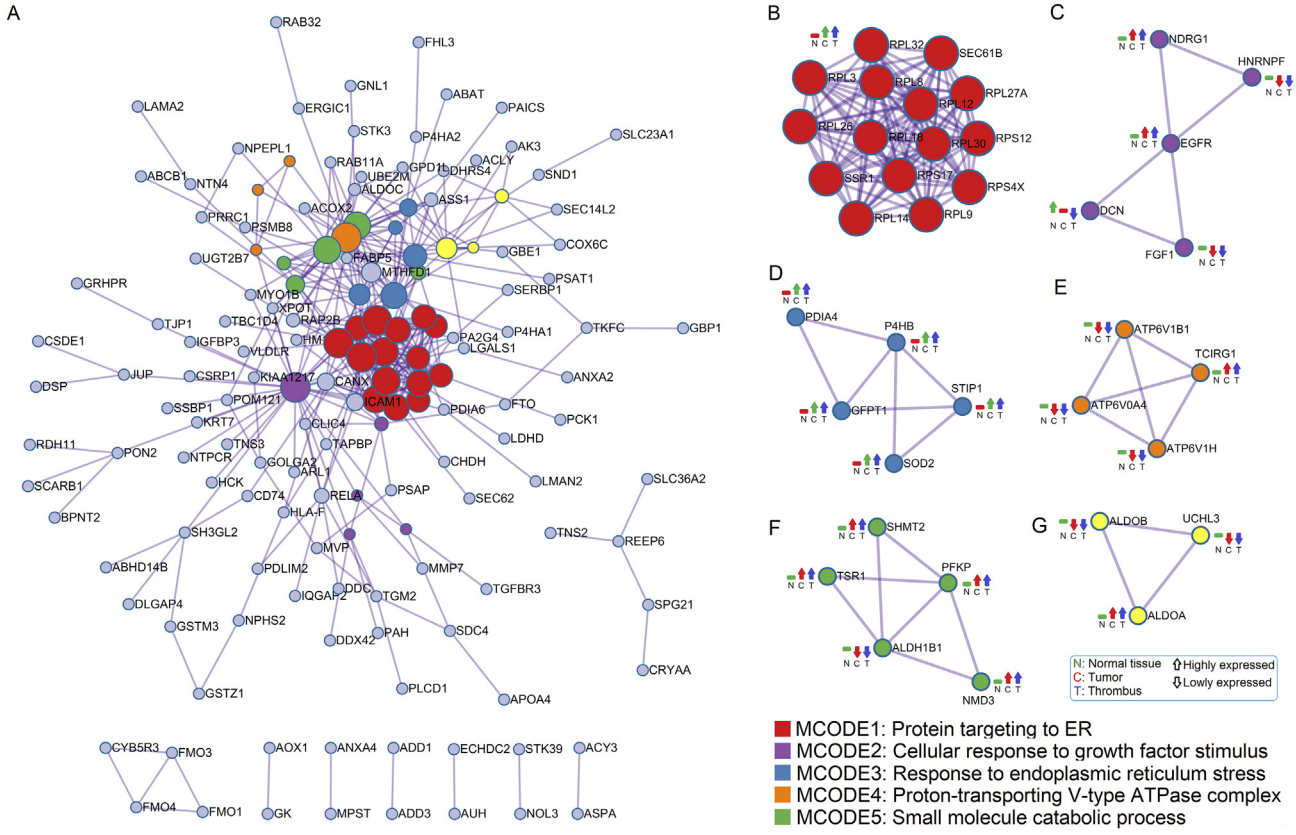

Fig. 5. Protein-protein interaction network and MCODE components. (A) Protein-protein interaction network constructed with all the dysregulated proteins among thrombus, tumor and normal tissue. Genes are presented as nodes and interactions are presented as edges. MCODE sub-networks are marked by colors. (B–G) Densely connected network components revealed by MCODE algorithm. Different tissue groups are marked by color and change trends are marked by arrow. Five MCODE components were revealed: Protein targeting to ER (C), cellular response to growth factor stimulus (D), response to endoplasmic reticulum stress (E), proton-transporting V-type ATPase complex (F) and small molecule catabolic process (G).

For the survival analysis, considering the fact that the transcriptome information of thrombus was not included in the TCGA database, we could not investigate the relationship between survival and thrombus status. Therefore, the survival analysis mainly focused on the correlation between prognosis and the mRNA expression levels of the dysregulated proteins in patients with ccRCC tumors. Apart from the ccRCC, we also included some type of urinary tumors and common tumors to obtain an overview of the tumor-type specificity of these proteins. As can be seen in the heat map, the prognosis correlation was mostly in accordance with the regulative trends of proteins in the proteomic result. Specifically, the downregulated proteins in the tumor presented a worse survival rate when the gene was less expressed in the tumor (hazard ratio less than 0, Fig. 6A), while the same pattern was observed for the upregulated proteins as well (Fig. 6B). Compared with the prognostic correlation of these genes in other tumor types, these genes presented obvious specificity, especially when compared with the non-urinary tract tumors such as those of lung, liver, pancreatic, and breast. PHYHD1 and CHDH were the only proteins with a prognostic correlation in the dysregulated protein clusters 1–5. These two proteins were downregulated in tumors compared to normal tissue, and the lower mRNA level correlated with a worse prognosis (Fig. 6D, F and G). However, the expression levels of these two proteins in the thrombus were higher than those in the tumor (Fig. 2). This result indicates that the worse prognosis of patients with venous thrombus may not be solely related to the malignancy of the thrombus cells because the biological features of thrombus, as illustrated in our present study, were in some aspects, similar to normal tissue instead of tumor tissue. Of course, our present study was preliminary and aimed to provide a global view of the different biological features among thrombus, tumor, and normal tissue. A more detailed experiment is needed before final conclusions can be made.

To validate the proteomic results, we chose three dysregulated proteins for the following reasons. First, the dysregulated proteins in clusters 1–5 were of great research value, so they were chosen for validation. However, considering the time consumption and expense for WB and IHC experiments, we could only choose some proteins (GGT5, KRT7, and CFHR1) as representatives for validation. Second, considering the accessibility and performance of the commercially available antibodies for WB and IHC, these three proteins were practical for validation. Third, the molecular functions of these three proteins were potentially related to tumor progression or poor survival (as discussed in the following paragraphs), which makes them meaningful for further detailed studies. The expression of these three proteins was verified by WB and IHC assays, and the results were in accordance with the proteomic results. In our study, GGT5 expression was downregulated in cancer tissues compared with that in normal kidney tissues. The tumor thrombus expressed the least amount of GGT5. We hypothesized that the upregulation of GGT5 could help to reduce the growth and progression of thrombus. However, as the regulation of GGT5 and its role in cancer remains unknown, further studies are required to investigate whether the altered GGT5 expression facilitates the invasion of the tumor into the vein. As mentioned before, GGT5 is a protein with enzymatic activity encoded by the GGT gene family. In addition, GGT1 is the only protein with enzymatic activity in this family and has physiological functions similar to those of GGT5. However, unlike GGT5, GGT1 has been widely investigated in tumors. Some studies have shown strong correlations between GGT1 expression and tumor progression or poor survival in breast, ovarian cancer, and some soft tissue sarcomas [26]. In addition, GGT1 was significantly downregulated in chromophobe RCC but not ccRCC, compared with normal kidney [27]. All these studies will guide further studies on GGT5 in RCC.

KRT7 had the same expression pattern as GGT5 in this study. Among the three types of tissues, the expression of KRT7 was lower in ccRCC cancer tissues and the least in thrombus tissues. An IHC study showed that the extent of KRT7 staining depended on the grade of ccRCC, those with the low-grade ccRCC expressed significantly higher levels of KRT7 than those of the high-grade ones [28]. This suggests that low KRT7 expression might correlate with a more malignant biological behavior. However, in this study, we investigated the expression of KRT7 in ccRCC with vena cava thrombus, to

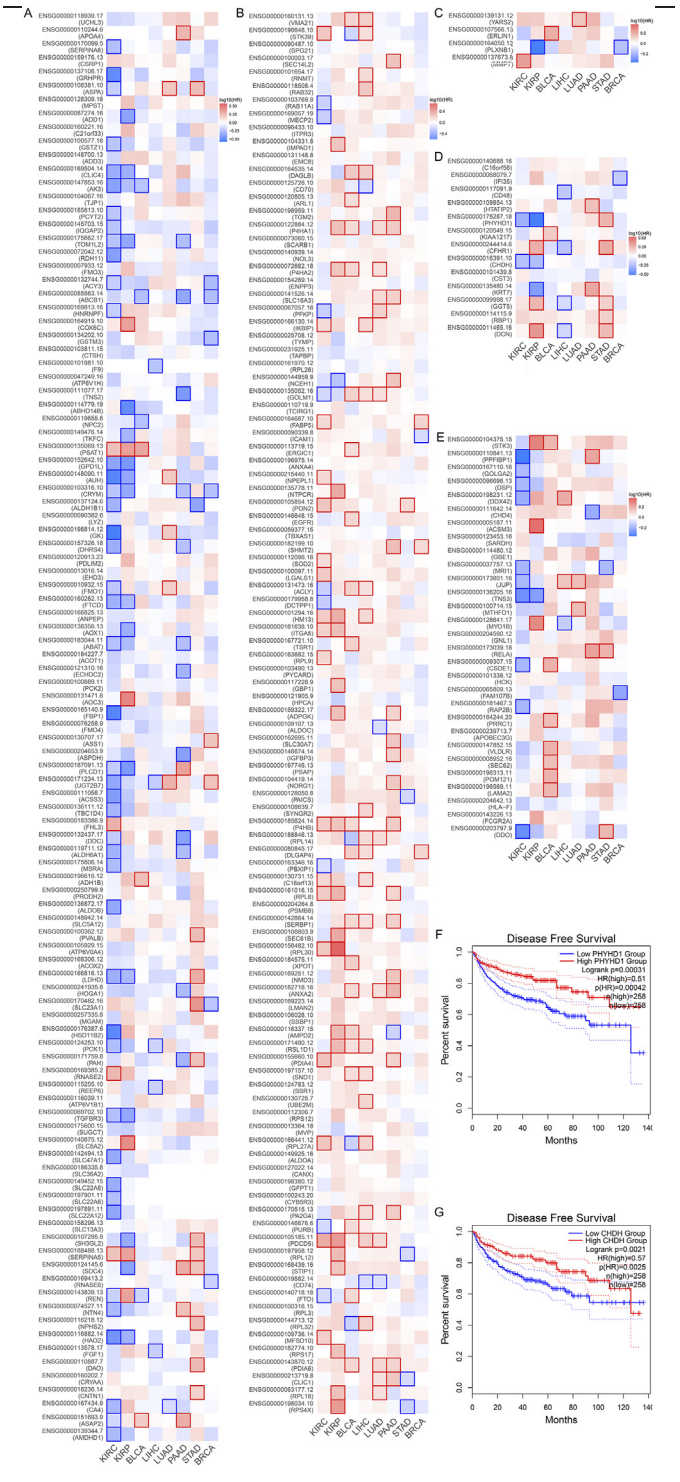

Fig. 6. Survival analysis for the dysregulated genes using TCGA database. (A–E) Heat map presenting the log10 (HR) of the genes in several type of tumors. A square with bold border represents a p value < 0.05 in the survival analysis. Results are presented separately in terms of changing trends: (A) Proteins that are highly expressed in normal tissue (dysregulated protein cluster 10). (B) Proteins that are lowly expressed in normal tissue (dysregulated protein cluster 11). (C) Proteins that changed only in thrombus (dysregulated protein cluster 6–7). (D) Proteins that changed in thrombus, tumor and normal tissue (dysregulated protein cluster 1–5). (E) Proteins that changed only in tumor (dysregulated protein cluster 8–9). (F–G) The K-M curves of PHYHD1 and CHDH. Abbreviations used: KIRC, kidney renal clear cell carcinoma; KIRP, kidney renal papillary cell carcinoma; BLCA, bladder urothelial carcinoma; LIHC, liver hepatocellular carcinoma; LUAD, lung adenocarcinoma; PAAD, pancreatic adenocarcinoma; STAD, stomach adenocarcinoma; BRCA, breast invasive carcinoma.

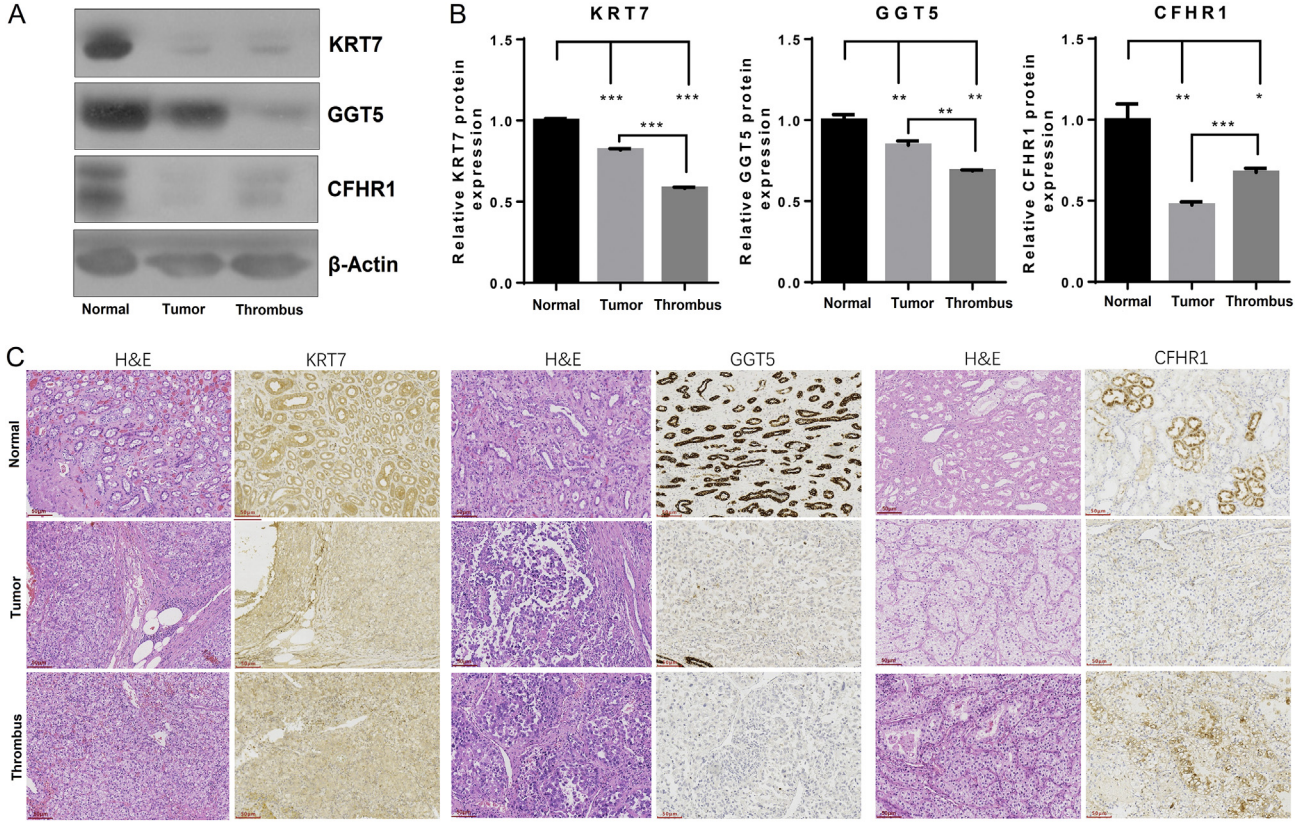

Fig. 7. Western blot and immunohistochemistry analysis of CFHR1, GGT5 and KRT7. (A) Examples for the western blot result of CFHR1, GGT5 and KRT7 from patient #5. (B) Statistical result of the western blot analysis of the three proteins in the validation cohort comprised of 15 ccRCC patients. The amount of target proteins are calculated by gray scanning and presented as column graph. (C) H&E staining and immunohistochemistry analysis result of the three proteins in thrombus, tumor and normal tissue. Group labels used: N, normal tissue; C, tumor; T, thrombus.

illustrate that KRT7 is a key molecule in ccRCC thrombus development. Our study found that the tumor thrombus expressed less KRT7 than the primary ccRCC, but the significance of this diversity is still unclear. We hypothesized that the tumor thrombus might be more aggressive than the primary ccRCC from which it grows.

Another important factor that might be involved in ccRCC thrombus formation is the human complement factor H-related protein 1 (CFHR1). CHFR1 inhibits the complement pathway by blocking C5 convertase activity and interfering with C5b surface deposition. Absent CFHR1 expression is related to age-related macular degeneration 1 and atypical hemolytic-uremic syndrome 1 [29]. However, its role in cancer is still largely unknown. A recent study has shown the function of CFHR1 in tumors: CFHR1 might potentially function as a tumor suppressor. The downregulation of CFHR1 was related to higher pathological T stage and shortened overall survival in patients with lung adenocarcinoma [30]. In this study, we also demonstrated the expression of CFHR1 in ccRCC tissues and thrombus tissues compared with normal kidney tissues, proving its important role in RCC thrombus formation. Further investigation is required to determine whether these changes of expression triggers or happens after tumor thrombus formation.

There are a few limitations to the present study. Due to the small sample size, it is not practical to compare the difference between patients in different disease stages, or with patients in stage 3/4 without tumor thrombus. It would also be meaningful to investigate the correlation between protein expression profiles and clinical outcomes. We would try to make a more detailed comparison and investigation of the dysregulated proteins between stages in a larger sample cohort in future studies.

In summary, this study employed comprehensive proteomic analysis for ccRCC thrombus and tumor tissues, providing valuable information for the distinctive molecular features and relevant pathways of thrombus. These findings are of great value and potential for further pathological researches or clinical applications.

Supplementary data to this article can be found online at https://doi.org/10.1016/j.tranon.2020.100895.

CRediT authorship contribution statement

Juntuo Zhou: Conceptualization, Methodology, Formal Analysis, Investigation, Writing - original draft. **Yimeng Song**: Conceptualization, Investigation, Writing - original draft, Funding acquisition. **Tianying Xing**: Investigation, Resources. **Liyuan Ge**: Investigation, Resources. **Lulin Ma**: Validation, Investigation. **Min Lu**: Conceptualization, Investigation, Writing - review and editing. **Lijun Zhong**: Conceptualization, Writing - review and editing, Supervision, Project administration.

Declaration of competing interest

The authors declare no potential conflicts of interest.

Acknowledgements

This study was supported by the Fund for Fostering Young Scholars of Peking University Health Science Center (Grant No. BMU2018PY006) and the National Natural Science Foundation of China (81500189).

Ethics approval and consent to participate

All procedures performed in studies involving human participants were in accordance with the ethical standards of the institutional and national

research committee of Peking University Third Hospital, and with the 1964 Helsinki declaration and its later amendments or comparable ethical standards. The ethical approval code was M2017147, and written informed consent was provided for all participants before enrollment.

Consent for publication

Written informed consent for publication was obtained from all participants.

Data availability statement

The raw MS data and MaxQuant processed result were deposited in MassIVE database with ID: MSV000085727. The datasets generated and analyzed during the current study are available from the corresponding author on reasonable request.

References

[1] K.W. Wong, Renal cell carcinoma with proliferative lupus nephritis, BMJ Case Rep. 2015 (2015).

[2] F. Hongo, N. Takaha, M. Oishi, T. Ueda, T. Nakamura, Y. Naitoh, Y. Naya, K. Kamoi, K. Okihara, T. Matsushima, S. Nakayama, H. Ishihara, T. Sakai, T. Miki, CDK1 and CDK2 activity is a strong predictor of renal cell carcinoma recurrence, Urol. Oncol. 32 (2014) 1240–1246.

[3] C. Coppin, C. Kollmannsberger, L. Le, F. Porzsolt, T.J. Wilt, Targeted therapy for advanced renal cell cancer (RCC): a Cochrane systematic review of published randomised trials, BJU Int. 108 (2011) 1556–1563.

[4] M. Jayson, H. Sanders, Increased incidence of serendipitously discovered renal cell carcinoma, Urology 51 (1998) 203–205.

[5] A. Seth, Management of IVC thrombus-surgical strategies and outcomes, Indian J. Surg. Oncol. 8 (2017) 156–159.

[6] M. Sun, L. Marconi, T. Eisen, B. Escudier, R.H. Giles, N.B. Haas, L.C. Harshman, D.I. Quinn, J. Larkin, S.K. Pal, T. Powles, C.W. Ryan, C.N. Sternberg, R. Uzzo, T.K. Choueiri, A. Bex, Adjuvant vascular endothelial growth factor-targeted therapy in renal cell carcinoma: a systematic review and pooled analysis, Eur. Urol. 74 (2018) 611–620.

[7] P. Ferronika, J. Hof, G. Kats-Ugurlu, R.H. Sijmons, M.M. Terpstra, K. de Lange, A. Leliveld-Kors, H. Westers, K. Kok, Comprehensive profiling of primary and metastatic ccRCC reveals a high homology of the metastases to a subregion of the primary tumour, Cancers (Basel) 11 (2019).

[8] X.M. Wang, Y. Lu, Y.M. Song, J. Dong, R.Y. Li, G.L. Wang, X. Wang, S.D. Zhang, Z.H. Dong, M. Lu, S.Y. Wang, L.Y. Ge, G.D. Luo, R.Z. Ma, S. George Rozen, F. Bai, D. Wu, L.L. Ma, Integrative genomic study of Chinese clear cell renal cell carcinoma reveals features associated with thrombus, Nat. Commun. 11 (2020) 739.

[9] M.A. Liss, Y. Chen, R. Rodriguez, D. Pruthi, T. Johnson-Pais, H. Wang, A. Mansour, D. Kaushik, Immunogenic heterogeneity of renal cell carcinoma with venous tumor thrombus, Urology 124 (2019) 168–173.

[10] M.A. Liss, Y. Chen, R. Rodriguez, D. Pruthi, T. Johnson-Pais, H. Wang, A. Mansour, J.R. White, D. Kaushik, Microbiome within primary tumor tissue from renal cell carcinoma may be associated with PD-L1 expression of the venous tumor thrombus, Adv. Urol. 2020 (2020) 9068068.

[11] E.C.B. Johnson, E.B. Dammer, D.M. Duong, L. Ping, M. Zhou, L. Yin, L.A. Higginbotham, A. Guajardo, B. White, J.C. Troncoso, M. Thambisetty, T.J. Montine, E.B. Lee, J.Q. Trojanowski, T.G. Beach, E.M. Reiman, V. Haroutunian, M. Wang, E. Schadt, B. Zhang, D.W. Dickson, N. Ertekin-Taner, T.E. Golde, V.A. Petyuk, P.L. De Jager, D.A. Bennett, T.S. Wingo, S. Rangaraju, I. Hajjar, J.M. Shulman, J.J. Lah, A.I. Levey, N.T. Seyfried, Large-scale proteomic analysis of Alzheimer's disease brain and cerebrospinal fluid reveals early changes in energy metabolism associated with microglia and astrocyte activation, Nat. Med. 26 (2020) 769–780.

[12] M. Matsumoto, F. Matsuzaki, K. Oshikawa, N. Goshima, M. Mori, Y. Kawamura, K. Ogawa, E. Fukuda, H. Nakatsumi, T. Natsume, K. Fukui, K. Horimoto, T. Nagashima, R. Funayama, K. Nakayama, K.I. Nakayama, A large-scale targeted proteomics assay resource based on an in vitro human proteome, Nat. Methods 14 (2017) 251–258.

[13] L. Zhong, J. Zhou, X. Chen, Y. Lou, D. Liu, X. Zou, B. Yang, Y. Yin, Y. Pan, Quantitative proteomics study of the neuroprotective effects of B12 on hydrogen peroxide-induced apoptosis in SH-SY5Y cells, Sci. Rep. 6 (2016) 22635.

[14] J.R. Wiśniewski, A. Zougman, N. Nagaraj, M. Mann, Universal sample preparation method for proteome analysis, Nat. Methods 6 (2009) 359–362.

[15] K.G. Danielson, H. Baribault, D.F. Holmes, H. Graham, K.E. Kadler, R.V. Iozzo, Targeted disruption of decorin leads to abnormal collagen fibril morphology and skin fragility, J. Cell Biol. 136 (1997) 729–743.

[16] I.T. Weber, R.W. Harrison, R.V. Iozzo, Model structure of decorin and implications for collagen fibrillogenesis, J. Biol. Chem. 271 (1996) 31767–31770.

[17] T. Neill, L. Schaefer, R.V. Iozzo, Decorin as a multivalent therapeutic agent against cancer, Adv. Drug Deliv. Rev. 97 (2016) 174–185.

[18] O. Binda, C. Nassif, P.E. Branton, SIRT1 negatively regulates HDAC1-dependent transcriptional repression by the RBP1 family of proteins, Oncogene 27 (2008) 3384–3392.

[19] M.H. Hanigan, E.M. Gillies, S. Wickham, N. Wakeham, C.R. Wirsig-Wiechmann, Immunolabeling of gamma-glutamyl transferase 5 in normal human tissues reveals that expression and localization differ from gamma-glutamyl transferase 1, Histochem. Cell Biol. 143 (2015) 505–515.

[20] P.H. Tan, L. Cheng, N. Rioux-Leclercq, M.J. Merino, G. Netto, V.E. Reuter, S.S. Shen, D.J. Grignon, R. Montironi, L. Egevad, J.R. Srigley, B. Delahunt, H. Moch, I.R.T. Panel, Renal tumors: diagnostic and prognostic biomarkers, Am. J. Surg. Pathol. 37 (2013) 1518–1531.

[21] A. Polistena, A. Cucina, S. Dinicola, C. Stene, G. Cavallaro, A. Ciardi, G. Orlando, R. Arena, G. D'Ermo, A. Cavallaro, L.B. Johnson, G. De Toma, MMP7 expression in colorectal tumours of different stages, In Vivo 28 (2014) 105–110.

[22] S. Giordano, S. Corso, P. Conrotto, S. Artigiani, G. Gilestro, D. Barberis, L. Tamagnone, P.M. Comoglio, The semaphorin 4D receptor controls invasive growth by coupling with Met, Nat. Cell Biol. 4 (2002) 720–724.

[23] D. Iacob, J. Cai, M. Tsonis, A. Babwah, C. Chakraborty, R.N. Bhattacharjee, P.K. Lala, Decorin-mediated inhibition of proliferation and migration of the human trophoblast via different tyrosine kinase receptors, Endocrinology 149 (2008) 6187–6197.

[24] K. Shostak, A. Chariot, EGFR and NF-κB: partners in cancer, Trends Mol. Med. 21 (2015) 385–393.

[25] R.R. Mohan, R. Tripathi, A. Sharma, P.R. Sinha, E.A. Giuliano, N.P. Hesemann, S.S. Chaurasia, Decorin antagonizes corneal fibroblast migration via caveolae-mediated endocytosis of epidermal growth factor receptor, Exp. Eye Res. 180 (2019) 200–207.

[26] M.H. Hanigan, Gamma-glutamyl transpeptidase: redox regulation and drug resistance, Adv. Cancer Res. 122 (2014) 103–141.

[27] C. Priolo, D. Khabibullin, E. Reznik, H. Filippakis, B. Ogorek, T.R. Kavanagh, J. Nijmeh, Z.T. Herbert, J.M. Asara, D.J. Kwiatkowski, C.L. Wu, E.P. Henske, Impairment of gamma-glutamyl transferase 1 activity in the metabolic pathogenesis of chromophobe renal cell carcinoma, Proc. Natl. Acad. Sci. U. S. A. 115 (2018) E6274–E6282.

[28] M.L. Gonzalez, R. Alaghehbandan, K. Pivovarcikova, K. Michalova, J. Rogala, P. Martinek, M.P. Foix, E.C. Mundo, E. Comperat, M. Ulamec, M. Hora, M. Michal, O. Hes, Reactivity of CK7 across the spectrum of renal cell carcinomas with clear cells, Histopathology 74 (2019) 608–617.

[29] S. Heinen, A. Hartmann, N. Lauer, U. Wiehl, H.M. Dahse, S. Schirmer, K. Gropp, T. Enghardt, R. Wallich, S. Halbich, M. Mihlan, U. Schlotzer-Schrehardt, P.F. Zipfel, C. Skerka, Factor H-related protein 1 (CFHR-1) inhibits complement C5 convertase activity and terminal complex formation, Blood 114 (2009) 2439–2447.

[30] G. Wu, Y. Yan, X. Wang, X. Ren, X. Chen, S. Zeng, J. Wei, L. Qian, X. Yang, C. Ou, W. Lin, Z. Gong, J. Zhou, Z. Xu, CFHR1 is a potentially downregulated gene in lung adenocarcinoma, Mol. Med. Rep. 20 (2019) 3642–3648.